島根大学地球資源環境学研究報告　22, 111～120 ページ（2003 年 12 月）
Geoscience Rept. Shimane Univ., 22, p.111～120（2003）

Article

Major and trace element abundances in the <180 μm fractions of stream sediments from the Kando River, Shimane Prefecture, Japan

Edwin Ortiz* and Barry Roser*

Abstract

Sieved fractions (<180 μm) of 86 stream sediment samples from active channels of the Kando River and its tributaries in east Shimane Prefecture were analyzed by X-ray fluorescence for major elements and 14 trace elements. Histograms of all data show that distributions are generally normal or are right-skewed to isolated higher values, as is typical for river sediments. Several elements (e.g. K_2O, Rb) have clearly bimodal distributions that are related to source. There is no evidence of anthropogenic impacts for elements which could be affected, such as P_2O_5, Cr, Ni or Pb. The results show clear contrasts in the composition of sediments collected upstream and downstream of the site of the Shitsumi dam. Those upstream are more aluminous, and tend to have greater abundances of K_2O, P_2O_5, MnO, Na_2O, Ba, Ce, Nb, Rb, Th, Y and Zr than those downstream. Conversely, Fe_2O_3T, TiO_2, Sc and V are generally more abundant in samples from below the dam site. These contrasts are related to source geology, with the catchment above the Shitsumi dam site being dominated by granitoids and felsic volcanic rocks, and that below by mixed volcanic and sedimentary rocks of the Hata, Kawai-Kuri and Omori Formations. The data clearly suggest that isolation of the upstream granitoid and felsic volcanic source terrane by closure of the Shitsumi dam will ultimately lead to more mafic compositions in stream sediments in the downstream reaches of the Kando River.

Key words: Geochemistry, stream sediments, <180 μm fraction, Kando River, Shimane

Introduction

Studies of chemical compositions of river and stream sediments provide key baseline data that can be utilized in a variety of geological and geoenvironmental studies. This report contains X-ray fluorescence (XRF) analyses of the <180 μm fraction from 86 stream sediment samples collected from the catchment of the Kando River, east Shimane Prefecture. The Kando catchment is located SW of Izumo City, and has an area of about 448 km^2 (Fig. 1). Study of the Kando catchment is of particular relevance because a high dam is currently being constructed at Shitsumi. This structure will eventually isolate part of the present catchment from the downstream areas, thus modifying the volume and characteristics of sediments reaching the Sea of Japan.

The purpose of this paper is to present the data obtained by XRF analysis, and to describe broad elemental abundances and variations of the fine fraction of sediments from the Kando River. Further and more detailed discussion of the results will be published elsewhere. The dataset reported here is intended to be used as comparative baseline data for similar studies of other river systems in the central San-in district, in addition to acting as a benchmark for measuring future change in the composition of the sediment in the Kando River after completion of the Shitsumi dam.

*Dept. of Geoscience, Shimane University, Matsue 690-8504, Japan

Geological Outline

Although the geology of the Kando River catchment is locally complex, at a regional scale it is relatively simple. Bedrock geology to the south (upstream) of the Shitsumi dam site is dominated by largely Paleogene to Cretaceous granitoids and felsic volcanic rocks (Fig. 1). The granitoids include granites, granites porphyries, granodiorites, gabbros, quartz diorites, and tonalites, whereas the volcanic rocks consist of rhyolite to dacite lava and pyroclastic rocks, and andesites (EBGMSP, 1997). In contrast, the downstream area to the north is a more complex assemblage of mainly Miocene rocks, principally of the Kawai-Kuri, Omori, Hata, Matsue and Fujina Formations (Fig.1). These lithostratigraphic units and their relations have been the subject of numerous studies with diverse foci (e.g. Takayasu, 1986; Kano *et al*. 1989; 1991; 1994; 1997; Morita & Nakayama, 1999; Roser *et al*., 2001). Lithotypes described in that area are varied, comprising basaltic to rhyolitic lavas and pyroclastic rocks, mafic intrusives, and locally derived sedimentary rocks, including sandstones, conglomerates and shales.

Several tributaries of the Kando River drain catchments consisting of dacite lavas and dacite pyroclastics from Mount Sanbe, located in the western central part of the catchment area. Other minor lithotypes including alkali basalt lava, dolerite, porphyrite, and Sangun Group basic and psammitic schist are scattered across the area.

A significant contrast in source rock compositions thus exists between the areas above and below the dam, in terms

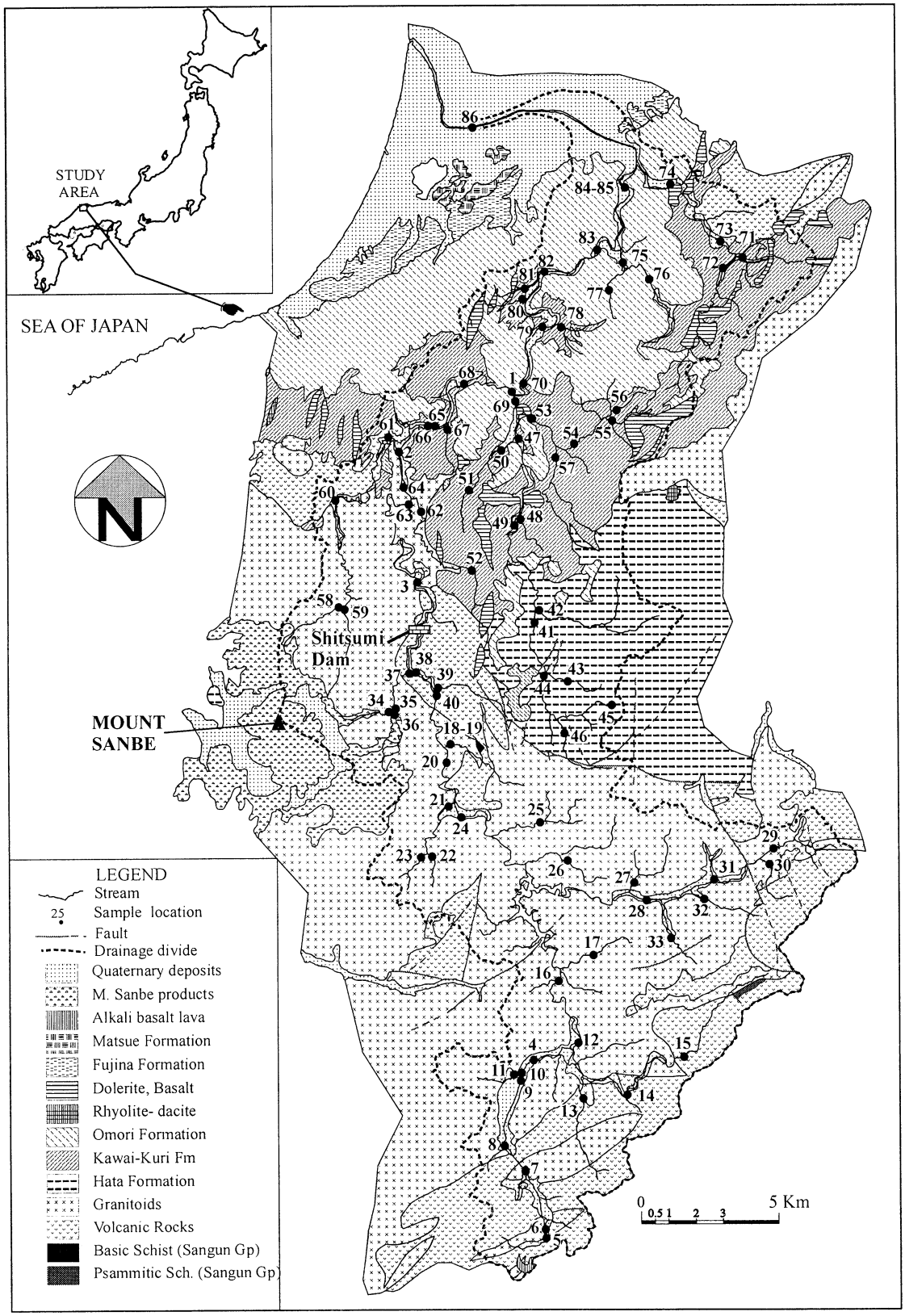

Fig. 1. Map showing the generalized distribution of lithotypes in the catchment of the Kando River and location of sample sites. Geology based on the 1:200,000 geological map of Shimane Prefecture (Editorial Board of the Geological map of Shimane Prefecture, 1997).

of both lithotype and chemistry. It is possible, therefore, that interruption of sediment flow down the Kando River by the Shitsumi dam will cause a change in the composition of both suspended sediment (very fine sand to mud) and coarser bedload (coarse to fine sand) in the downstream areas.

Sampling and Sample Preparation

Field sampling

Sampling was conducted on eight days during autumn 2002 (Sept. 25, Oct. 1, 9, 23, 25, 29, Nov. 8, 12). On all except one day weather was fine, and streams were clear and low. Rain fell on Nov. 8th (samples K 65-77), stream levels were raised by 10-20 cm, and waters were slightly turbid. Samples were collected with a plastic water scoop, from active channels. Sub-samples taken over a channel length of 20-50 m were combined as single samples and stored in plastic zip-top bags. Where possible, both sides of streams were sampled.

Samples sites were selected using a 1:50,000 topographic base map, to which geology had been added from the 1: 200,000 geological map of Shimane Prefecture (EBGMSP, 1997). Site selection was based on areal coverage, and with the aim of sampling representative drainages containing the range of lithotypes seen in the area. A number of samples were also collected from the main channel, downstream to near the mouth of the river. Sample locations are given in Figure 1, numbered in order of collection.

Sampling was not possible at some intended sites due to lack of sand or silt-sized material, particularly in upland areas. At a number of localities, samples could not been taken exactly where desired due to lack of access, as many smaller channels were fully-confined by steep concrete walls. In some cases channel floors were also concreted, and no samples could be collected. Lack of fines in channels between successive dams or weirs at some sites also meant that samples had to be taken from standing water behind these structures, rather than from freely flowing channels. A total of 86 samples were collected, representing a sampling density of one sample/5.2 km^2. This density is considered acceptable for the nature of the study.

Sample preparation

Bulk samples collected the day before were placed in stainless trays, and dried in a drying cabinet at 80-90℃. Each sample was then passed through a stainless steel mesh sieve to remove granules and pebbles coarser than 2 mm. That fraction was weighed and retained. The <2 mm fraction was then weighed. Total sample weights were generally between 1000 and 1500 g, averaging 1235 g. The <2 mm fraction was split into quarters or eighths using a simple alumina chute. Depending on size and silt content, a quarter or eighth split (half for 2 samples) was then hand sieved through an 83 mesh stainless steel sieve to separate sufficient <180 μm material (c. 5-20 g) for XRF analysis. On average, the <180 μm fraction comprised 13.4% of the material <2 mm. Only in nine samples did the <180 μm fraction comprise 30% or more.

The <180 μm fractions were then ground in an automatic agate pestle and mortar for 15 minutes, and a 7-8 g sub-sample placed in glass vials. These sub-samples were then dried at 110℃ for at least 24 h prior to determination of loss on ignition (LOI).

Analytical Methods

Gravimetric LOI determinations were made by weighing the dried samples into ceramic crucibles, followed by ignition in a muffle furnace at 1000℃ for at least two hours. LOI was then calculated from the net weight loss. The ignited material was then manually disaggregated or re-crushed in an agate pestle and mortar, and returned to a 110 ℃ oven for at least 24 hours. This ignited material was used for preparation of the fusion beads for X-ray fluorescence analysis (anhydrous basis).

Analyses of major elements and 14 trace elements (Ba, Ce, Cr, Ga, Nb, Ni, Pb, Rb, Sc, Sr, Th, V, Y, Zr) were made using a Rigaku RIX-2000 XRF at Shimane University. All analyses were performed on glass beads prepared in an automatic bead sampler (fusion 240 seconds, agitation 360 seconds), using an alkali flux comprising 80% lithium tetraborate and 20% lithium metaborate, with a sample to flux ratio of 1:2. Analytical methods, instrumental conditions and calibration follow those described by Kimura and Yamada (1996). Analyses were monitored by repeat analyses of seven GSJ and USGS standards, from new beads not included in the original calibration. The results were verified by cross-calibration against the recommended values for those seven standards. Additional descriptions of the general methods used are given in Roser *et al*. (2000, 2001).

Results and Discussion

The <180 μm fraction XRF data are listed on a hydrous basis in Table 1. LOI contents were generally low to moderate (<10%), but sporadic high values >10% were observed, due to the presence of significant quantities of organic matter in some samples. Many of the samples with elevated LOI values were collected from sites behind small dams or weirs. Organic matter may be especially significant in these samples. This will be verified by CHNS analysis. However, some high values were also recorded from open channel sites (Table 1).

Elemental abundances show considerable ranges, even after normalization to 100% anhydrous to eliminate the effect of varying LOI (Table 2). The average composition over the entire suite is similar to that of average Upper Continental Crust, except for depletion in Nb and slight

Table 1. Major and trace element analyses of the <180 μm fractions, Kando River (hydrous basis). Major element values weight per cent, trace element values p.p.m.

SaNr	TYPE	SiO_2	TiO_2	Al_2O_3	Fe_2O_3T	MnO	MgO	CaO	Na_2O	K_2O	P_2O_5	LOI	Total	Ba	Ce	Cr	Ga	Nb	Ni	Pb	Rb	Sc	Sr	Th	V	Y	Zr
K1	MCB	62.93	1.08	14.32	8.33	0.18	1.18	3.04	2.83	1.95	0.11	3.57	99.52	348	46	37	17	7	15	24	58	14.2	286	5.7	220	17	222
K2	MCB	61.74	1.06	15.21	8.98	0.19	1.29	3.21	3.21	2.11	0.14	2.85	99.99	348	67	28	18	10	8	28	70	11.1	422	10.0	209	19	365
K3	MCB	63.40	0.67	15.77	5.53	0.14	1.14	3.26	3.08	2.35	0.13	3.97	99.43	358	52	13	18	7	8	19	83	10.2	460	9.4	107	18	246
K4	A	57.59	1.07	16.20	10.58	0.27	1.03	2.17	2.52	2.58	0.17	6.09	100.25	426	105	33	20	14	12	20	95	12.7	226	20.9	169	35	622
K5	A	56.97	1.54	14.46	11.34	0.25	1.41	2.21	1.58	2.40	0.15	7.23	99.53	446	77	99	19	14	41	16	97	12.2	251	14.6	295	25	407
K6*	A	55.81	0.87	15.37	6.93	0.20	1.06	1.82	1.28	2.44	0.21	13.97	99.97	504	65	96	17	11	43	11	107	11.6	214	11.7	141	24	226
K7	A	56.03	1.43	14.88	12.11	0.32	0.97	1.82	1.95	2.46	0.19	7.49	99.65	422	120	53	19	15	13	14	96	12.6	194	28.3	237	33	395
K8	A	60.68	0.66	16.26	6.86	0.33	0.88	1.82	1.99	2.89	0.19	7.62	100.18	475	60	30	18	10	18	25	117	10.5	207	12.8	99	25	264
K9*	A	53.09	0.62	17.86	7.08	0.14	0.99	1.63	1.54	2.23	0.35	14.54	100.08	452	59	34	17	10	14	7	100	12.2	167	12.0	92	33	190
K10	A	58.03	0.64	17.10	6.74	0.45	1.01	2.15	2.10	2.36	0.27	9.34	100.19	477	64	48	19	10	26	19	97	10.8	226	12.7	87	28	257
K11	A	57.41	0.84	16.60	9.49	0.35	1.12	2.45	2.73	2.33	0.15	6.25	99.72	453	105	47	18	11	21	18	78	10.9	286	22.9	155	30	858
K12	A	61.03	0.86	16.39	7.30	0.25	1.15	2.53	2.58	2.95	0.15	4.77	99.97	487	61	77	18	6	43	27	105	14.3	256	10.6	146	22	248
K13*	A	57.39	0.44	17.10	5.26	0.26	0.75	1.70	2.21	3.14	0.18	11.46	99.91	543	69	54	15	8	32	8	114	7.2	195	18.8	68	22	190
K14	A	59.37	0.82	15.66	6.11	0.16	1.04	2.52	2.19	2.39	0.16	9.82	100.23	411	62	33	17	10	14	13	89	13.4	282	10.3	135	29	213
K15*	A	54.61	0.53	15.20	4.28	0.12	0.84	2.02	1.79	2.44	0.19	17.53	99.55	392	59	21	16	10	12	10	103	8.6	234	11.0	71	29	173
K16	A	58.04	1.07	16.08	9.03	0.26	1.23	2.64	2.52	2.44	0.20	6.51	100.03	400	68	54	18	10	24	21	90	14.9	269	12.8	203	25	325
K17	A	55.33	0.51	20.08	4.88	0.19	1.13	2.97	3.09	2.10	0.16	9.28	99.72	415	73	25	20	10	17	10	87	11.3	399	15.5	63	29	243
K18	A	59.28	0.83	15.86	7.70	0.23	1.25	2.79	2.98	2.24	0.15	6.57	99.87	366	57	51	19	9	29	40	89	11.6	304	10.0	184	28	219
K19	A	60.53	0.46	16.30	4.51	0.24	0.98	2.60	2.62	2.52	0.13	8.48	99.36	392	57	69	17	9	48	33	98	8.8	366	10.1	59	20	178
K20	A	57.77	0.93	15.99	8.72	0.34	1.30	2.94	2.80	2.24	0.17	6.68	99.88	417	66	35	18	10	15	27	83	13.1	358	13.5	174	25	384
K21	A	57.70	0.52	16.22	5.77	0.48	0.96	2.30	2.40	2.34	0.21	10.71	99.62	462	49	18	17	8	13	15	85	9.2	332	8.6	60	22	194
K22	A	53.29	0.58	16.11	6.93	0.64	0.99	2.39	2.20	2.14	0.24	14.54	100.04	438	47	17	17	8	12	8	78	8.5	327	8.5	86	23	210
K23	A	50.98	0.40	15.90	5.70	0.51	0.84	2.35	1.84	2.08	0.25	18.71	99.55	413	70	22	12	9	17	4	84	7.3	268	13.6	55	38	167
K24	A	62.80	0.70	16.42	5.67	0.23	1.14	2.98	3.57	2.46	0.12	3.81	99.90	365	68	16	18	9	8	29	91	12.5	379	12.4	106	27	335
K25*	A	50.56	0.39	17.40	4.85	0.18	0.95	2.52	2.37	2.08	0.23	18.47	100.00	388	60	17	15	9	10	6	89	8.8	350	13.1	59	30	153
K26	A	56.31	0.55	18.68	6.30	0.30	1.24	2.81	3.23	2.35	0.20	8.38	100.35	419	82	28	20	10	16	16	92	11.2	397	16.8	74	32	383
K27	A	47.15	2.06	14.28	21.05	0.43	1.28	2.15	2.63	1.93	0.18	5.66	98.79	431	123	55	21	22	15	21	66	12.0	259	16.9	438	29	1642
K28	A	59.29	0.60	16.32	7.02	0.36	1.05	2.67	3.37	2.54	0.21	6.66	100.08	446	84	57	18	10	35	18	91	10.4	322	17.4	108	29	325
K29*	A	54.75	0.66	16.73	6.28	0.24	1.28	2.72	2.43	2.11	0.23	12.43	99.85	419	65	26	17	9	15	15	74	12.7	325	9.8	120	24	316
K30	A	54.00	0.57	18.06	4.68	0.17	1.12	2.26	2.23	2.13	0.36	14.64	100.20	432	59	59	17	10	24	11	81	11.8	303	10.0	85	24	202
K31*	A	57.12	0.59	17.39	6.21	0.23	1.18	2.57	2.66	2.40	0.23	9.32	99.90	466	57	38	19	9	22	22	86	13.4	331	9.5	89	23	252
K32	A	56.90	0.53	16.62	7.74	0.34	0.99	2.90	3.13	2.18	0.25	8.73	100.30	415	117	88	17	7	52	12	74	11.9	354	12.0	95	21	225
K33	A	56.80	0.58	17.60	6.15	0.17	1.22	3.14	3.35	2.32	0.15	8.39	99.88	393	73	48	19	9	27	12	78	10.2	405	14.6	100	21	327
K34	A	60.20	0.46	16.77	5.14	0.23	1.41	4.78	3.62	1.56	0.29	5.30	99.76	386	49	78	17	8	49	16	48	7.8	782	5.8	74	12	181
K35	A	63.19	0.38	17.33	3.84	0.13	1.28	4.63	3.87	1.71	0.18	2.24	98.79	411	42	15	19	7	12	34	51	7.0	783	5.7	48	11	132
K36	A	64.02	0.40	17.25	4.05	0.14	1.28	4.32	3.85	1.81	0.21	2.45	99.77	427	46	79	18	7	51	33	55	6.5	733	6.9	49	11	138
K37	A	60.11	0.43	16.25	4.53	0.20	1.25	4.43	3.55	1.71	0.23	5.71	98.41	403	48	81	17	7	52	16	53	8.1	703	5.4	67	13	162
K38	A	60.70	0.93	15.59	8.13	0.25	1.25	3.04	2.99	2.27	0.12	4.58	99.86	402	69	36	19	10	17	27	80	10.3	380	11.1	178	23	360
K39	A	59.04	0.69	15.65	5.97	0.18	0.99	2.47	2.18	2.06	0.12	10.62	99.96	380	51	43	17	8	24	17	79	9.8	335	8.2	132	17	244
K40	A	61.88	0.65	16.26	5.78	0.22	1.15	2.81	3.08	2.36	0.14	5.63	99.94	415	59	32	18	9	18	30	86	10.9	376	11.8	110	21	265
K41	B	60.30	1.00	16.65	8.28	0.22	1.53	3.20	2.52	1.62	0.12	4.65	100.08	326	41	28	20	7	15	21	56	20.9	355	6.5	214	21	188
K42	B	59.75	0.83	16.15	7.77	0.23	1.25	3.06	1.98	1.42	0.14	7.39	99.98	347	50	47	19	7	23	17	47	16.4	321	5.9	183	23	209
K43	B	58.60	0.79	18.44	6.50	0.18	1.09	2.22	1.68	1.35	0.12	9.21	100.18	356	42	16	20	7	9	15	49	16.8	318	5.6	143	21	160
K44	B	58.88	0.81	17.50	7.77	0.32	1.42	2.85	2.32	1.76	0.14	6.32	100.10	394	47	47	20	7	26	25	65	19.3	330	8.1	162	22	194
K45*	B	56.76	0.63	18.70	5.13	0.16	1.12	2.60	1.99	1.30	0.23	11.52	100.12	366	43	20	20	7	12	18	42	15.2	405	5.7	99	18	137
K46	B	59.21	0.57	18.50	5.70	0.26	1.03	2.57	3.00	2.69	0.10	6.63	100.24	389	66	42	22	10	23	19	110	9.5	356	16.1	98	30	241
K47	B	61.87	0.95	15.21	8.28	0.20	1.35	2.47	2.37	1.65	0.14	5.35	99.84	353	39	50	18	7	27	20	55	17.8	270	6.0	212	20	165
K48	B	60.61	1.12	15.61	8.59	0.20	1.22	1.53	1.86	1.09	0.16	8.15	100.12	304	38	33	18	5	14	19	40	20.5	193	4.4	239	23	161
K49	B	59.97	1.29	15.40	10.05	0.19	1.43	2.87	2.23	1.46	0.12	4.90	99.91	324	48	55	20	7	30	23	47	20.8	313	6.4	305	19	197
K50	B	62.91	1.33	13.87	9.82	0.20	1.06	1.66	2.12	1.44	0.11	5.55	100.08	307	48	40	18	7	17	20	50	16.9	194	6.2	264	19	207

Table 1 (ctd).

SaNr	TYPE	SiO_2	TiO_2	Al_2O_3	Fe_2O_3T	MnO	MgO	CaO	Na_2O	K_2O	P_2O_5	LOI	Total	Ba	Ce	Cr	Ga	Nb	Ni	Pb	Rb	Sc	Sr	Th	V	Y	Zr
K51	B	61.51	1.28	15.38	9.72	0.25	1.19	1.87	2.04	1.40	0.13	5.50	100.24	315	41	45	19	7	22	19	41	16.2	194	4.6	228	23	175
K52	B	58.49	1.03	16.51	9.05	0.38	1.09	2.00	1.84	1.55	0.19	8.20	100.34	423	56	42	20	9	21	16	59	15.4	289	7.9	212	22	239
K53	B	61.36	1.48	13.93	11.02	0.19	1.08	1.68	2.13	1.93	0.14	5.01	99.95	403	47	134	18	7	60	23	63	16.2	181	6.5	321	18	192
K54*	B	60.39	0.88	16.14	6.80	0.18	1.17	1.74	1.71	1.21	0.15	10.11	100.46	323	43	20	18	6	13	12	46	18.8	197	5.9	157	22	252
K55	B	65.00	1.15	14.53	7.51	0.16	1.09	1.60	1.67	1.39	0.10	5.96	100.15	312	42	29	17	7	13	20	51	17.5	194	4.8	216	18	211
K56	B	62.52	0.86	14.84	7.40	0.14	1.30	1.53	1.79	1.40	0.13	8.39	100.30	308	38	34	17	6	19	12	58	18.0	172	5.2	174	17	161
K57	B	66.00	0.71	14.17	6.02	0.16	0.91	1.53	2.38	2.44	0.12	5.65	100.09	381	41	30	16	6	13	16	85	14.2	195	5.2	139	16	160
K58	B	61.17	0.50	17.93	5.16	0.31	1.05	3.39	3.29	2.37	0.17	5.12	100.47	449	56	24	19	9	17	23	75	7.8	551	11.4	69	13	237
K59	B	58.87	0.67	16.88	6.66	0.18	1.32	4.05	3.24	1.83	0.24	6.20	100.13	396	57	43	19	9	23	21	56	10.0	641	7.1	119	13	300
K60	B	60.60	0.82	16.18	8.93	0.16	1.16	3.64	3.37	2.02	0.21	3.20	100.30	378	71	31	20	10	17	25	60	13.3	585	11.5	168	15	445
K61	B	64.42	0.51	16.65	4.29	0.15	1.09	3.46	3.39	2.18	0.16	3.36	99.66	393	48	17	18	8	10	33	65	8.1	587	6.8	72	13	158
K62	B	62.93	0.81	16.28	6.36	0.14	1.36	2.25	3.09	2.17	0.15	4.79	100.34	324	61	28	19	10	11	35	88	15.1	315	10.8	133	23	195
K63	MCB	61.45	0.64	16.31	5.86	0.16	1.25	2.99	2.95	2.33	0.18	6.09	100.19	429	53	61	19	9	35	23	82	11.9	421	9.0	109	20	207
K64	MCB	58.64	0.96	15.46	9.59	0.27	1.30	2.60	2.90	2.40	0.20	5.77	100.11	408	67	77	20	11	36	25	85	12.6	336	13.5	209	24	293
K65	MCB	64.40	0.74	16.00	5.98	0.11	1.26	3.25	3.18	2.10	0.13	2.95	100.11	365	47	16	19	8	8	31	70	10.1	456	7.3	133	17	233
K66	MCB	63.35	0.70	16.46	5.50	0.11	1.29	3.27	3.24	2.12	0.13	4.08	100.24	366	55	21	19	9	11	32	72	8.0	484	8.7	124	17	233
K67	B	59.75	1.00	16.84	8.12	0.17	1.48	2.26	1.76	1.14	0.14	7.55	100.23	312	40	10	19	6	10	17	35	20.9	202	4.2	204	20	172
K68	MCB	60.94	0.86	16.13	7.24	0.17	1.33	3.13	2.83	1.98	0.16	5.52	100.28	380	55	27	19	9	11	31	66	10.9	403	8.9	167	21	258
K69	B	63.32	0.82	15.32	7.13	0.11	1.28	2.12	2.39	1.74	0.14	5.91	100.26	364	41	48	18	6	23	19	58	16.1	237	5.6	162	21	146
K70	MCB	61.72	1.27	14.35	10.26	0.17	1.23	2.42	2.46	1.68	0.12	4.26	99.94	338	44	37	18	8	12	20	54	16.4	267	6.1	302	19	251
K71	B	55.89	1.81	16.47	11.76	0.30	1.68	2.87	2.27	1.23	0.12	5.68	100.08	355	47	53	20	8	17	21	37	20.3	238	5.6	362	20	323
K72	B	59.90	1.08	15.81	8.73	0.13	1.54	2.61	2.09	1.57	0.13	6.65	100.25	324	40	19	19	6	9	16	51	21.6	193	5.6	241	22	181
K73	B	61.25	1.22	15.22	9.00	0.15	1.37	2.62	2.16	1.62	0.14	5.33	100.07	355	38	29	18	7	12	20	52	18.1	209	5.8	257	21	203
K74	B	60.19	0.92	16.38	7.52	0.12	1.40	2.84	2.20	1.60	0.16	7.05	100.38	352	41	28	18	7	10	18	54	20.0	212	5.9	192	21	159
K75	B	61.40	0.87	14.72	7.26	0.18	1.05	2.14	2.18	1.48	0.14	8.87	100.29	357	35	39	17	6	19	19	41	16.7	172	4.6	164	19	182
K76	B	65.12	0.79	14.70	6.82	0.18	0.94	2.04	2.21	1.56	0.12	5.66	100.15	353	36	52	16	5	31	15	45	16.3	173	4.2	159	18	179
K77	B	57.47	1.82	14.14	12.26	0.21	1.03	2.30	2.36	1.36	0.15	6.75	99.83	344	37	70	19	9	29	19	32	17.9	174	4.4	365	19	289
K78	B	57.53	0.90	15.03	8.30	0.26	1.59	2.22	1.50	1.45	0.15	11.37	100.30	370	32	44	17	5	25	18	36	21.1	177	2.2	213	20	128
K79	MCB	62.23	0.86	15.22	7.26	0.17	1.26	2.66	2.62	1.78	0.15	5.99	100.21	362	46	60	17	7	33	23	59	14.5	304	5.9	171	20	203
K80	B	59.09	0.86	16.31	7.32	0.09	1.90	2.96	1.95	1.55	0.14	8.09	100.28	470	30	37	18	6	19	22	49	19.1	269	3.9	163	18	132
K81	B	56.51	0.95	14.89	7.74	0.14	1.57	2.31	1.63	1.32	0.15	12.58	99.78	408	41	30	17	6	14	10	42	20.2	228	4.0	190	20	150
K82	MCB	61.51	0.94	15.57	7.68	0.19	1.36	2.71	2.58	1.84	0.16	5.76	100.31	379	52	47	19	8	24	28	62	15.7	322	7.9	193	19	194
K83	MCB	61.76	1.34	14.62	9.96	0.19	1.45	3.26	2.88	1.76	0.12	2.67	100.00	333	48	25	19	8	10	26	55	17.6	369	7.0	301	19	287
K84	MCB	61.24	0.70	15.68	6.22	0.20	1.22	2.52	2.33	1.75	0.17	8.32	100.34	376	41	58	17	7	29	14	59	15.6	272	5.9	131	21	166
K85	MCB	59.96	0.70	15.74	6.28	0.17	1.23	2.37	2.16	1.71	0.18	9.71	100.18	373	44	40	17	7	21	16	59	13.8	250	5.8	133	22	166
K86	MCB	62.99	0.84	15.92	6.99	0.14	1.38	3.05	2.72	1.86	0.14	3.95	99.98	357	46	15	18	7	8	24	61	15.2	357	6.6	155	18	240

Notes: SaNr= Sample number. TYPE= Catchment type; A-above dam site; B-secondary drainages below dam site; MCB- main channel below dam site.

LOI= loss on ignition. Astered samples were collected from behind weirs.

Table 2. Summary statistics for all <180 μm fraction samples (anhydrous normalized data). N = 86.

Element	Mean	Min	Max	SDp
Major elements (wt%)				
SiO_2	64.23	50.63	69.89	2.46
TiO_2	0.92	0.39	2.21	0.35
Al_2O_3	17.43	14.67	22.20	1.58
Fe_2O_3T	8.04	3.98	22.60	2.53
MnO	0.24	0.10	0.75	0.11
MgO	1.30	0.85	2.06	0.20
CaO	2.83	1.62	5.06	0.68
Na_2O	2.70	1.49	4.01	0.59
K_2O	2.14	1.18	3.55	0.50
P_2O_5	0.18	0.11	0.42	0.06
Trace elements (ppm)				
Ba	422.7	324.5	614.2	61.1
Ce	60.9	33.0	132.0	20.4
Cr	45.1	10.8	141.3	23.9
Ga	19.7	15.1	23.5	1.3
Nb	9.1	5.2	23.9	2.7
Ni	23.1	7.9	63.6	12.8
Pb	21.3	5.0	42.7	7.3
Rb	75.7	34.4	129.1	23.9
Sc	14.7	6.7	23.7	4.3
Sr	349.6	182.9	828.2	142.2
Th	10.1	2.4	30.7	5.1
V	172.1	49.9	470.5	83.4
Y	23.6	11.6	46.8	6.4
Zr	275.7	136.3	1762.7	196.1

Min Minimum
Max Maximum
SDp Population standard deviation

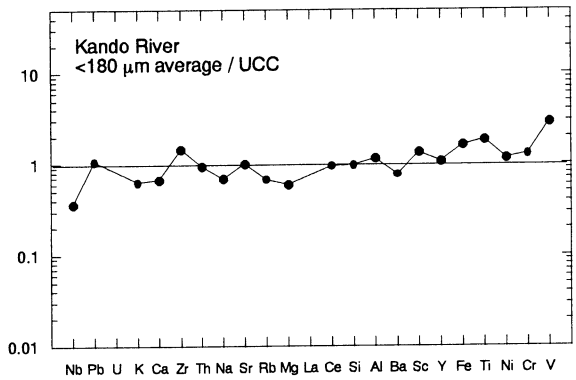

Fig. 2. Multi-element plot showing the average composition (anhydrous normalized) of the <180 μm fractions from the Kando River (data from Table 2) normalized against the Upper Continental Crust (UCC) average of Taylor & McLennan (1985). Elements are arranged from left to right in order of increasing normalized abundance in average Mesozoic-Cenozoic greywacke (Condie 1993) relative to UCC, following the methodology of Dinelli *et al*. (1999). The major elements are normalized as oxides.

enrichment in Zr (Fig. 2). The largest departure from UCC composition is seen among the elements linked with mafic minerals phases or mafic igneous detritus, which increase from left to right in the segment Sc-V.

Histograms of anhydrous-normalized major element abundances show the data for a number of elements (SiO_2 (Fig. 3a), Fe_2O_3T, MnO, P_2O_5) resemble normal distributions, but all show some anomalous values. One sample (K 27) has very low SiO_2 (50.63%), which is caused by marked enrichment in Fe_2O_3T (22.60%), TiO_2 (2.21%), and MnO (0.46%), presumably through Fe-Ti-Mn oxide heavy mineral concentration or authigenic crust material. MnO (Fig. 3b) and TiO_2 are strongly skewed to higher values, as is P_2O_5. The distribution of K_2O is clearly bimodal (Fig. 3c); this may also be the case for MgO and CaO. Al_2O_3 (Fig. 3d) and Na_2O contents show considerable variation, with polymodal distributions and skew to higher values.

Among the trace elements, two elements (Ba (Fig.4a), Pb) show relatively normal distributions, with little evidence of skewing or anomalous values. The remainder show moderate or marked skew to higher values. This is most pronounced for Ce, Cr, Ni, Th, V, and Zr (Fig. 4b), for which a small number of samples have contents more than two standard deviations from the mean. The most anomalous values for Zr (1762 ppm), V (471 ppm), Ce (132 ppm) are seen in sample K 27, which also has the extreme values of Fe, Ti and Mn, as noted above. The distribution of the Rb data is clearly bimodal (Fig 4c), with the two modes split almost equally about the mean. Weak tendency for polymodality is also seen in the Ga (Fig. 4d), Nb, and Sr distributions.

The results of this study provide baseline data for the <180 μm fraction of stream sediments from the Kando River. The generally normal, right-skewed distributions are typical of fractions taken from river sediments. Most of the elements analyzed to date are not prone to major disturbances from anthropogenic sources, with the possible exception of P_2O_5 (from fertilizer), and metallic elements such as Cr, Ni, and Pb. The abundances of all four of these elements are unexceptional, and hence there is no clear evidence of influence from human activity. The compositions observed thus primarily reflect that of the source rock types, and of the soils developed on them. Skewed distributions are predictable, as are occasional anomalous values exceeding two standard deviations from the mean. In this case, anomalous values of Fe, Mn, Ti, Ce, Cr, Ni, Th, V, Y and Zr are most likely due to concentrations of high-density accessory minerals. Probable phases involved include the Fe-Ti oxides which formed the basis of the historic iron industry in the area (Fe, Ti, Cr, Ni, V), fragments of authigenic or pedogenic Fe-Mn oxide coatings, and heavy minerals such as zircon and apatite (Ce, Th, Y, Zr) that occur in the granitoids. High values for each of these groups are commonly contained in single samples.

Heavy mineral concentration cannot, however, explain

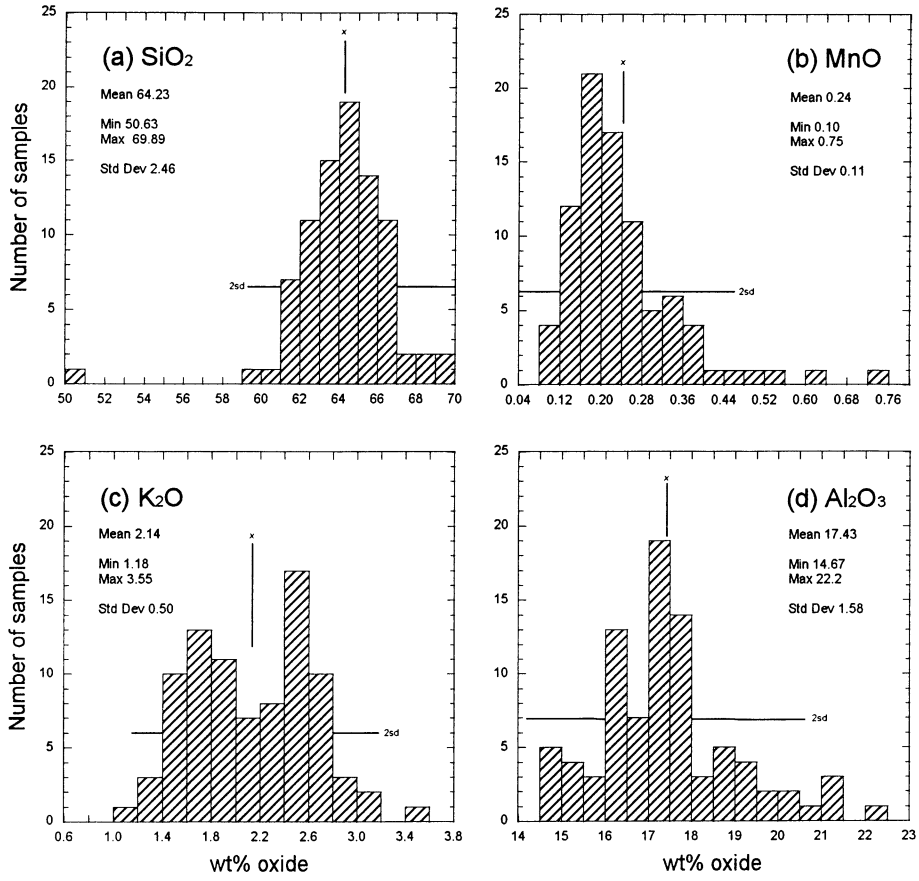

Fig. 3. Examples of histograms of major element abundances (anhydrous normalized data) in the <180 μm fraction, Kando River. Min = minimum; Max = maximum; Std Dev = standard deviation; vertical bar x = mean; horizontal bar (2 sd) = ±2 standard deviations from the mean. (a) SiO_2–normal distribution; (b) MnO–skewed to higher values; (c) K_2O–bimodal; (d) Al_2O_3–considerable variation with polymodality and skew to higher values.

the tendency for bimodality seen for some elements, such as Mg, K, Ga, and Rb, which are normally concentrated in clays or low-density silicate phases. Such elements are more likely to be controlled by the composition of source lithotypes. The Kando catchment is almost equally divided between Paleogene to Cretaceous granitoids and felsic volcanics in the south, and a mixed assemblage of Hata, Kawai-Kuri and Omori Formation volcanics and sediments in the north, along with small amounts of mafic rocks. Consequently, the watershed above the new dam site is primarily felsic, and that below somewhat more mafic. As a first step in examining the influence of source rock lithotype, we have divided the sample sites into three categories:

(1). Sites above the dam site (all sites upstream of Site 3), representing the total catchment for the new dam.

(2). Main channel sites below the dam site (3, 63, 64, 2, 66, 65, 68, 1, 79, 82, 83, 84-86), which now carry granitoid-derived material originating from above site 3, and material from secondary catchments below the dam site.

(3). Secondary drainages below the dam site. These catchments will form the main source of sediment after completion of the dam.

Simple element-Al_2O_3 variation diagrams reveal significant differences in the chemistry of the samples in each category. The first feature of the major elements is that the <180 μm fractions above the dam site are generally more aluminous (>17 wt%) than those in the main channel or in the secondary drainages below the dam site (Fig. 5). Although there is little difference in CaO (Fig. 5a) and MgO between the three categories, some contrasts are evident for the remaining major elements, although overlap is considerable. Fe_2O_3T (Fig. 5b), TiO_2, and to a lesser extent SiO_2 are generally more abundant in samples from below the dam site, especially when Al_2O_3 contents are low (< 17%). Main channel samples below site 3 tend to have intermediate values. In contrast, K_2O, P_2O_5 (Fig. 5c; d), MnO and to some extent Na_2O show greater values above the dam site. Main channel samples are again intermediate.

Trace element abundances also show some clear contrasts between the groups. Th, Rb (Fig. 6a; b), Ba, Ce, Nb, Y and Zr show clear enrichment in the fractions collected above

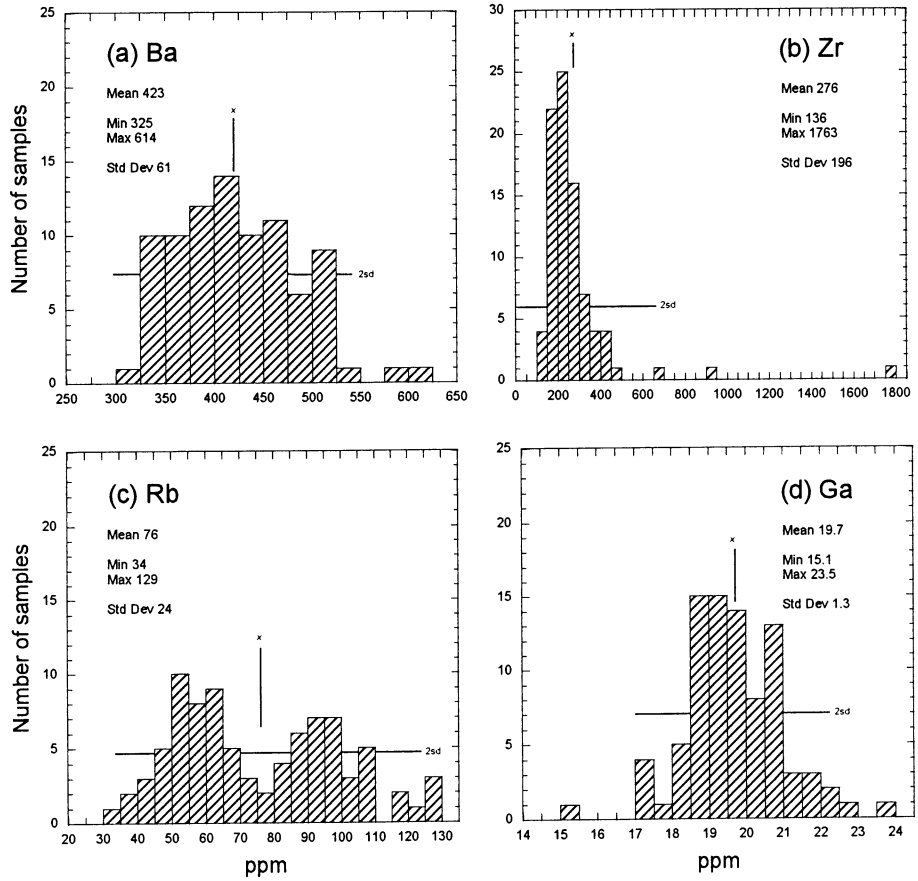

Fig. 4. Examples of histograms of trace element abundances (anhydrous normalized data) in the <180 μm fraction, Kando River. Min = minimum; Max = maximum; Std Dev = standard deviation; vertical bar x = mean; horizontal bar (2 sd) = ±2 standard deviations from the mean. (a) Ba and (b) Zr–relatively normal distributions with skew to higher values; (c) Rb–bimodal; (d) Ga–polymodal.

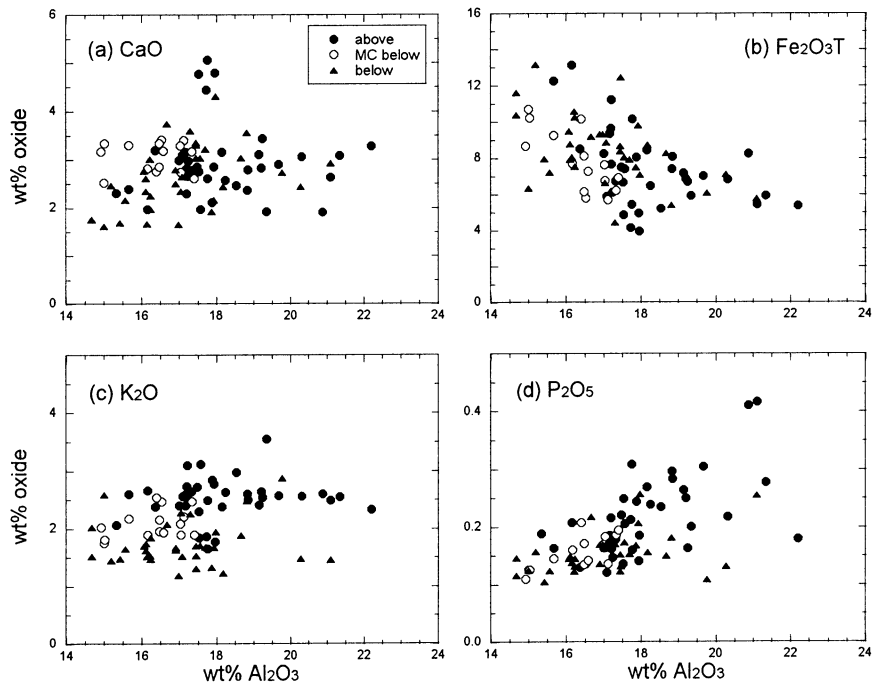

Fig. 5. Examples of major element-Al_2O_3 variations in the <180 μm fraction (anhydrous normalized data), Kando River, according to position with respect to the dam site. MC below = main channel below the dam site. (a) CaO–little difference between groups; (b) Fe_2O_3T–greater abundances in samples from below the dam site; (c) K_2O and (d) P_2O_5–greater abundances in samples from above the dam site.

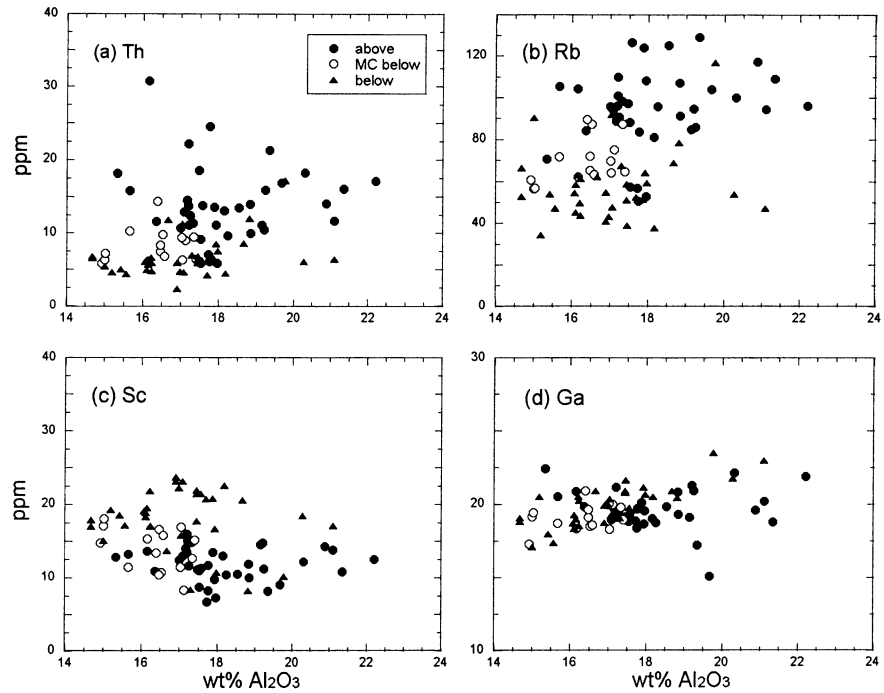

Fig. 6. Examples of trace element-Al_2O_3 variations in the <180 μm fraction (anhydrous normalized data), Kando River, according to position with respect to the dam site. MC below = main channel below the dam site. (a) Th and (b) Rb–greater abundances in samples from above the dam site; (c) Sc–greater abundances in samples from below the dam site; (d) Ga–little difference between groups.

the dam site. This association of elements is compatible with the granitoid and felsic volcanic source at these sites, and the greater concentration of K_2O in the samples of this group. Contents of Cr, Ni, and Sr also tend to be a little greater in that group, but the distinction is not as clear-cut. In the secondary drainages below the dam site, Sc (Fig. 6c) and V abundances are clearly greater than those above the dam site or in the main channel, consistent with their enrichment in Fe_2O_3T and TiO_2. Only Ga (Fig. 6d) and Pb show little contrast between the three groups.

In all the variation diagrams, samples from the main channel fall between the distributions of those from above and below the dam site. This reflects mixing of detritus derived from the lithologically varied catchments in the lower area with granitoid-felsic volcanic detritus derived from upstream. This and the clear associations of elements with each group suggest that source lithotype is the main determinant of bulk composition.

Conclusions

Bulk chemical compositions of <180 μm fractions in sediments from the Kando River and its tributaries reflect the nature of their source lithotypes. A clear contrast in composition exists between sediments derived from granitoids and felsic volcanics in the south (upstream of the Shitsumi dam site) with those from more varied and more mafic lithotypes (Hata, Kawai-Kuri and Omori Formations) in the north. Isolation of the felsic catchments in the south by completion of the Shitsumi dam will inevitably lead to a shift in the composition of sediments in the Kando River below the dam site, toward a more mafic character.

Acknowledgements

This work was part of a collaborative project with The Tokuoka Laboratory for Study of Brackish Water Environments, Matsue. Our thanks to Takao Tokuoka for suggesting the project and for facilitating it, and to Masami Saito (Tokuoka Laboratory) for her help with administration. We are also grateful to Miwa Akashi and Minoru Oono of Takeshita Engineering Consultant Co. for their invaluable assistance during field work.

References

Condie, K. C. 1993: Chemical composition and evolution of the upper continental crust: Contrasting results from surface samples and shales. *Chemical Geology*, **104**, 1-37.

Dinelli, E.; Lucchini, F.; Mordenti, A.; Paganelli, L. 1999: Geochemistry of Oligocene-Miocene sandstones of the northen Apennines (Italy) and evolution of chemical features in relation to provenance changes. *Sedimentary Geology*, **127**, 193-207.

Editorial Board of Geological map of Shimane Prefecture (EBGMSP) 1997. Geological map of Shimane Prefecture (1:200,000).

Kano, K., Takeuchi, K., Oshima, K. and Bunno, M. 1989. Geology of the Taisha district. With geological sheet map at a scale of 1:50,000. Tsukuba, Geological Survey of Japan, 30 p.*

Kano, K., Takeuchi, K., and Matsuura, H. 1991. Geology of the Imaichi district. With geological sheet map at a scale of 1:50,000. Tsukuba, Geological Survey of Japan, 79 p.*

Kano, K., Yamauchi, S., Takayasu, K., Matsuura, H. and Bunno, M. 1994. Geology of the Matsue district. With geological sheet map at a scale of 1: 50,000. Tsukuba, Geological Survey of Japan, 126 p.*

Kano, K., Matsuura, H., Sawada, Y., and Takeuchi, K. 1997. Geology of the Iwami-Oda and Oura districts. With geological sheet map at a scale of 1: 50,000. Tsukuba, Geological Survey of Japan, 118 p.*

Kimura, J.-I. and Yamada, Y. 1996. Evaluation of major and trace element analyses using a flux to sample ratio of two to one glass beads. *Journal of Mineralogy, Petrology and Economic Geology*, **91**, 62-72.

Morita, H. and Nakayama, K. 1999. Stratigraphy of the Middle Miocene in southwestern part of Izumo City in Shimane Prefecture of SW Japan, and subsiding properties of its sedimentary basin. *Geoscience Reports of Shimane University*, **18**, 25-39.*

Roser, B.P., Tateishi, Y. and Nakayama, K. 2001. Whole-rock geochemical compositions of Miocene sedimentary and volcanic rocks from the Izumo -Matsue districts and Shimane Peninsula, SW Japan. *Geoscience Reports of Shimane University*, **20**, 69-82.

Roser, B.P., Kimura, J.-I., and Hisatomi, K. 2000. Whole-rock elemental abundances in sandstones and mudrocks from the Tanabe Group, Kii Peninsula, Japan. *Geoscience Reports of Shimane University*, **19**, 101-112.

Takayasu, K. 1986. Diversification in the molluscan fauna of the Miocene Izumo Group, San-in district, southwest Japan. *Paleontological Society of Japan Special Paper*, **29**, 173-186.

Taylor, S. R. and McLennan, S. M. 1985. *The continental crust: its composition and evolution*. Oxford, Blackwell Scientific, 312 pp.

* In Japanese, English abstract or summary

(Received: Oct. 31, 2003, Accepted: Dec. 12, 2003)

（要　旨）

エドウィン・オルティス，バリー・P・ロザー，2003，島根県神戸川における＜180 μm 画分河川堆積物の主成分微量成分組成，島根大学地球資源環境学報告，22, 111-120.

神戸川とその支流から 86 の堆積物試料を採取し，180 μm 画分を篩い分けて XRF 分析を行った．全体の組成は河川堆積物に特徴的な元素分布を示すが，K_2O や Rb についてはバイモーダルな分布を示した．組成は志津見ダムの上流と下流で顕著な差を示す．下流の組成はより塩基性成分が卓越することを示している．このダムの上流には酸性の珪長質岩が分布し，下流には波多・川合－久利，大森層の中性火山岩が露出する．志津見ダムによって上流の酸性火山岩フラックスが下流で妨げられていることが，下流域の塩基性成分の富化の原因であると結論づけられる．